

AD-A161 900

PICOSECOND OPTOELECTRONIC MEASUREMENT OF MICROSTRIP  
DISPERSION. (U) AEROSPACE CORP EL SEGUNDO CA CHEMISTRY  
AND PHYSICS LAB D E COOPER 30 SEP 85

1/1

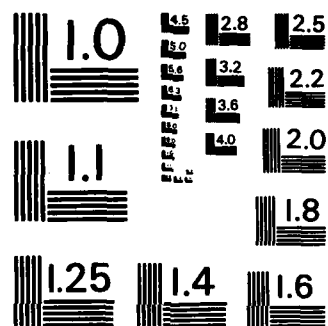
UNCLASSIFIED

TR-0084A(5945-06)-1 SD-TR-85-72

F/G 9/5

ML





MICROCOPY RESOLUTION TEST CHART  
NATIONAL BUREAU OF STANDARDS-1963-A

12

AD-A161 980

## Picosecond Optoelectronic Measurement of Microstrip Dispersion

D. E. COOPER  
Chemistry and Physics Laboratory  
Laboratory Operations  
The Aerospace Corporation  
El Segundo, CA 90245

30 September 1985

APPROVED FOR PUBLIC RELEASE;  
DISTRIBUTION UNLIMITED

DTIC  
ELECTE  
DEC 6 1985  
S A D

NTC FILE COPY

Prepared for

SPACE DIVISION  
AIR FORCE SYSTEMS COMMAND  
Los Angeles Air Force Station  
P.O. Box 92960, Worldway Postal Center  
Los Angeles, CA 90009-2960

85 12 6 105

This report was submitted by The Aerospace Corporation, El Segundo, CA 90245, under Contract No. F04701-83-C-0084 with the Space Division, P.O. Box 92960, Worldway Postal Center, Los Angeles, CA 90009-2960. It was reviewed and approved for The Aerospace Corporation by S. Feuerstein, Director, Chemistry and Physics Laboratory. Lieutenant Carl Baner, SD/CGX, was the project officer for the Mission-Oriented Investigation and Experimentation (MOIE) program.

This report has been reviewed by the Public Affairs Office (PAS) and is releasable to the National Technical Information Service (NTIS). At NTIS, it will be available to the general public, including foreign nationals.

This technical report has been reviewed and is approved for publication. Publication of this report does not constitute Air Force approval of the report's findings or conclusions. It is published only for the exchange and stimulation of ideas.



CARL BANER, Lt, USAF  
MOIE Project Officer  
SD/CGX



JOSEPH HESS, GM-15  
Director, AFSTC West Coast Office  
AFSTC/WCO OL-AB

## UNCLASSIFIED

SECURITY CLASSIFICATION OF THIS PAGE (When Data Entered)

REPORT DOCUMENTATION PAGE		READ INSTRUCTIONS BEFORE COMPLETING FORM
1. REPORT NUMBER SD-TR-85- 72	2. GOVT ACCESSION NO. AD-A161 980	3. RECIPIENT'S CATALOG NUMBER
4. TITLE (and Subtitle) Picosecond Optoelectronic Measurement of Microstrip Dispersion		5. TYPE OF REPORT & PERIOD COVERED
		6. PERFORMING ORG. REPORT NUMBER TR-0084A(5945-06)-1
7. AUTHOR(s) D. E. Cooper	8. CONTRACT OR GRANT NUMBER(s) F04701-83-C-0084	
9. PERFORMING ORGANIZATION NAME AND ADDRESS The Aerospace Corporation El Segundo, CA 90245		10. PROGRAM ELEMENT, PROJECT, TASK AREA & WORK UNIT NUMBERS
11. CONTROLLING OFFICE NAME AND ADDRESS Space Division Los Angeles Air Force Station Los Angeles, CA 90009-2960		12. REPORT DATE 30 September 1985
		13. NUMBER OF PAGES 13
14. MONITORING AGENCY NAME & ADDRESS (if different from Controlling Office)		15. SECURITY CLASS. (of this report) Unclassified
		15a. DECLASSIFICATION/DOWNGRADING SCHEDULE
16. DISTRIBUTION STATEMENT (of this Report) Approved for public release; distribution unlimited.		
17. DISTRIBUTION STATEMENT (of the abstract entered in Block 20, if different from Report)		
18. SUPPLEMENTARY NOTES		
19. KEY WORDS (Continue on reverse side if necessary and identify by block number) Picosecond                      Dispersion Optoelectronic                  Propagation Microstrip                        Microwave		
20. ABSTRACT (Continue on reverse side if necessary and identify by block number) The broadening and distortion of 5-psec electrical pulses propagating on microstrip lines were measured. The dispersion curve of the microstrip was measured with a 150-GHz bandwidth. Comparison with an approximate analytical dispersion formula indicates that the microstrip is much less dispersive than expected.		

## PREFACE

The author gratefully acknowledges J. Ewan and D. Rowe for helpful discussions in interpreting the experimental results.

Accession For	
NTIS CRA&I	<input checked="checked" type="checkbox"/>
DTIC TAB	<input type="checkbox"/>
Unannounced	<input type="checkbox"/>
Justification	
By	
Distribution/	
Availability Codes	
Dist	Avail and/or Special
A1	



## CONTENTS

PREFACE.....	1
I. INTRODUCTION.....	7
II. EXPERIMENTAL.....	9
III. RESULTS.....	11
IV. DISCUSSION.....	13
V. SUMMARY.....	17
REFERENCES.....	19

## FIGURES

1. Electrical pulse shape with no propagation and after  
1.3 cm propagation..... 12
2. Microstrip dispersion curves..... 16

## I. INTRODUCTION

Very short electrical pulses can be produced by optically triggering optoelectronic switches incorporated into microstrip transmission lines.<sup>1</sup> However, microstrip dispersion causes short electrical pulses to broaden and distort as they propagate. Conventional continuous-wave (cw) dispersion measurements on microstrips<sup>2</sup> have been limited to 18-GHz bandwidth. Here we report optoelectronic generation and sampling of electrical pulses with 5-psec temporal resolution and the use of these pulses to probe dispersion effects of the high-frequency microstrip propagation modes.<sup>3</sup> Theoretical calculations of the dispersed pulse shapes were performed by Whinnery and coworkers;<sup>4</sup> our results confirm their predictions. Fourier analysis of the dispersed pulse shapes yields the microstrip dispersion curve to about 150 GHz. The measured curve is much less dispersive than an approximate analytical dispersion curve,<sup>5</sup> which may be due to the small dimensions of the microstrips used.

## II. EXPERIMENTAL

Microstrip circuits incorporating optoelectronic switches were fabricated on silicon-on-sapphire wafers. The substrate was 180  $\mu\text{m}$  thick, with a 1.0- $\mu\text{m}$  epilayer of silicon. The microstrip lines were formed with 150 nm of evaporated gold; they were 180  $\mu\text{m}$  wide to provide for 50  $\Omega$  impedance. The microstrip circuit consisted of a central microstrip and four side microstrips oriented 90 deg to the central strip. A 25- $\mu\text{m}$  gap between each side strip and the central strips acted as an optoelectronic switch to generate and sample electrical pulses. The four switches were arranged to permit sampling of the pulse shape after it had propagated immediately across the microstrip and after propagation distances of 6.5 and 13 mm. The wafers were ion implanted with 400 keV  $\text{Si}^+$  to shorten the duration of the photoconductive response into the picosecond regime. A dose of  $7 \times 10^{14} \text{ cm}^{-2}$  was adequate for optimal temporal response; smaller doses produced greater photoconductivity with a reduction in temporal resolution.

A quasi-cw train of 3-psec optical pulses from a synchronously pumped dye laser was focused onto a biased optoelectronic switch to produce short electrical pulses on the central microstrip. As the voltage pulse propagated past one of the other optoelectronic switches it caused a transient bias, which could be detected by illumination of the switch with a second picosecond laser pulse. In this way the switches operated as sampling gates: The aperture was swept by delaying the second optical pulse. The current conducted by the sampling switch was amplified and used to drive the Y axis of an XY recorder. The X axis was driven by a voltage proportional to the position of the optical delay line, and the result was a record of the temporal profile of the electrical pulse.

### III. RESULTS

Figure 1(a) shows the result of sampling the electrical pulse immediately across the microstrip from the generation site, corresponding to an optoelectronic autocorrelation function. The superimposed points are a fitted Gaussian profile. To the right of the main peak is a small shoulder, probably caused by the electromagnetic wave radiated from the biased switch reflecting off the ground plane and modulating the bias on the sampling switch.<sup>6</sup> Aside from this shoulder the autocorrelation profile is quite symmetric and fairly close to a Gaussian shape. The symmetry is not expected, since the discharging of one switch and charging of the second switch should produce an asymmetric signal shape.<sup>6</sup> Indeed, the minor asymmetry near the peak of the pulse does appear to be reproducible. However, if we neglect this asymmetry and assume that the 7.0-psec-wide signal results from the convolution of a Gaussian electrical pulse with a Gaussian sampling aperture, the electrical pulse width (and sampling aperture) can be inferred to be 5.0 psec. A 5.0-psec pulse has a frequency spectrum with a half-power width of 62 GHz.

Figure 1(b) shows the electrical pulse profile after 1.3 cm propagation on the microstrip. The pulse becomes distorted because low frequencies propagate on the microstrip in a nearly transverse electromagnetic (quasi-TEM) mode in which part of the electric field passes through the air above the dielectric substrate, resulting in an effective dielectric constant  $\epsilon_{re}$  that is considerably less than the substrate dielectric constant  $\epsilon_r$ .<sup>7</sup> As the frequency increases the quasi-TEM mode begins to couple to the  $TE_1$  surface wave mode that propagates at the dielectric-air interface, but mostly within the dielectric.<sup>3</sup> The mixed propagation mode possesses a larger effective dielectric constant, ultimately reaching the high-frequency effective dielectric constant  $\epsilon_r$ . Thus, low-frequency components of the electrical pulse travel relatively fast and form the slowly rising leading edge of the pulse. The high-frequency components become concentrated in the trailing edge of the pulse and cause the observed oscillation. The data reported here represent the first observation of the reversed polarity region at the trailing edge of the pulse.

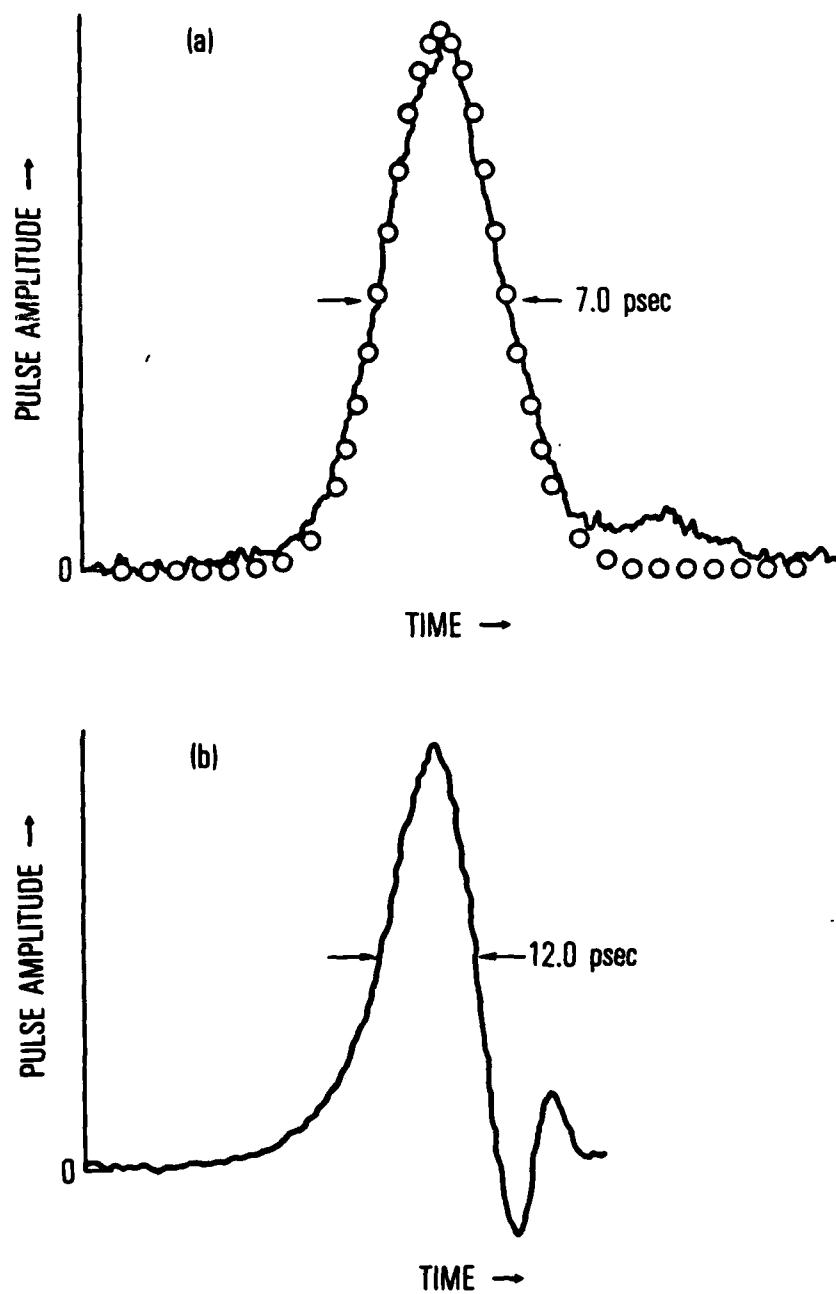


Fig. 1. Electrical pulse shape (a) with no propagation (superimposed points are a Gaussian fit); and (b) after 1.3 cm propagation.

#### IV. DISCUSSION

The amplitude and phase of the frequency spectrum of the pulse profiles measured at different points along the microstrip conductor can be obtained by Fourier analysis. Microstrip losses affect the amplitude of the transformed pulse spectrum, whereas microstrip dispersion affects the phase components. Here we consider the frequency spectrum of the pulse as it propagates on the microstrip line and the limitation imposed by sampling with a finite (and possibly asymmetric) aperture.

The temporal profile of the signal resulting from optoelectronic sampling of an electrical pulse propagating on the microstrip is the convolution of the pulse profile and the sampling aperture:

$$V(t;l) = P(t;l)*S(t) = P(t;0)*I(t;l)*S(t) \quad (1)$$

where  $V(t;l)$  is the temporal profile of the signal after propagation over distance  $l$ ,  $P(t;l)$  is the electrical pulse profile at point  $l$ , and  $S(t)$  is the sampling aperture profile. The symbol  $*$  denotes the convolution operation. The right-hand side of Eq. (1) applies the fact that the pulse profile at point  $l$  is the convolution of the initial pulse profile  $P(t;0)$  and the impulse response function  $I(t;l)$  for a section of microstrip of length  $l$ .

If we use the properties of the Fourier transforms of convolutions,<sup>8</sup> Eq. (1) can be written (using the "bar" notation to indicate a Fourier transform)

$$\overline{V(f;l)} = \overline{P(f;l)} \times \overline{S(f)} = \overline{P(f;0)} \times \overline{T(f;l)} \times \overline{S(f)} \quad (2)$$

This is the form that is useful for analyzing the dispersed pulse profiles.  $\overline{T(f;l)} = \overline{I(f;l)}$ , the transfer function for transmission through a length  $l$  of microstrip, completely describes the electrical properties of the microstrip (in a linear approximation).

The initial pulse  $P(t;0)$  will generally have an exponential tail due to the exponentially decaying photoconductivity response after optical

excitation. The resulting asymmetry in  $P(t;0)$  is equivalent to a frequency-dependent phase angle in  $\overline{P(f;0)}$ . The sampling aperture will be approximately equal to the time-reversed initial pulse profile:

$$S(t) \approx P(-t;0) \quad (3)$$

If this approximation holds, then  $V(t;0)$  is an autocorrelation function and it will be completely symmetric. The symmetry of Fig. 1(a) indicates that Eq. (3) is a good approximation. Then the phase angles of  $\overline{S(f)}$  will be equal and opposite those of  $\overline{P(f;0)}$ , and any nonzero phase components of  $\overline{V(f;l)}$  must be due to  $T(f;l)$  [Eq. (2)]. Thus the asymmetry in the sampling aperture exactly compensates for an identical asymmetry in the initial pulse, and the microstrip dispersion is measured directly.

Microstrip dispersion can be expressed as a variation in propagation constant  $\beta = 2\pi/\lambda$  with frequency. The ratio between the propagation constant on the microstrip and the propagation constant in vacuum  $\beta_0$  is equal to the square root of the effective dielectric constant  $\epsilon_{re}$ :

$$\frac{\beta(f)}{\beta_0} = \epsilon_{re}^{1/2}(f) = \frac{\lambda_0}{\lambda(f)} = \frac{c}{f\lambda(f)} \quad (4)$$

where  $\lambda_0$  is the wavelength in vacuum.

The phase angle (in radians) of a wave propagating along a microstrip will equal the distance propagated  $l$  times the propagation constant  $2\pi/\lambda$ :

$$\phi(f) = \frac{2\pi l}{\lambda(f)} \quad (5)$$

Substituting Eq. (4) into Eq. (5), we solve for the effective dielectric constant

$$\epsilon_{re}^{1/2}(f) = \phi(f) \frac{c}{2\pi l} \frac{1}{f} \quad (6)$$

Equation (6) enables the dispersion function  $\epsilon_{re}^{1/2}(f)$  to be calculated from the phase information in  $T(f;l)$ . The low-frequency limit of  $\epsilon_{re}$  is determined by

the arrival time of the pulse (112 psec), and the dispersion curve is calculated from Eq. (6) and the frequency-dependent phase angles of  $T(f;l)$ .

The dispersed pulse shape of Fig. 1(b) was digitized and analyzed with a fast Fourier transform routine on a microcomputer. The  $\epsilon_{re}^{1/2}$  was calculated from the transform phase components and Eq. (6), and the results are plotted in Fig. 2 (dotted curve). The data indicate a smooth frequency dependence to as high as 150 GHz, where the noise starts to grow because of the small amplitude of these frequency components. In fact the amplitude of the 150-GHz component is less than  $10^{-3}$  that of the dc component, so the excellent frequency bandwidth of the data testifies to the good signal-to-noise properties of the picosecond optoelectronic data.

Also plotted in Fig. 2 is the dispersion curve calculated from an approximate analytical equation (solid curve).<sup>5</sup> The parameters used to calculate this curve are the microstrip dimensions and the sapphire dielectric constant perpendicular to the substrate, which is 9.95 for the sapphire orientation used here. Clearly, the observed dispersion is much flatter than that expected at lower frequencies, which may indicate that the cutoff frequency for the  $TE_1$  surface wave mode is higher than expected for these small ( $w=h=180\text{ }\mu\text{m}$ ) microstrip structures. We are proceeding with further investigations of this problem.

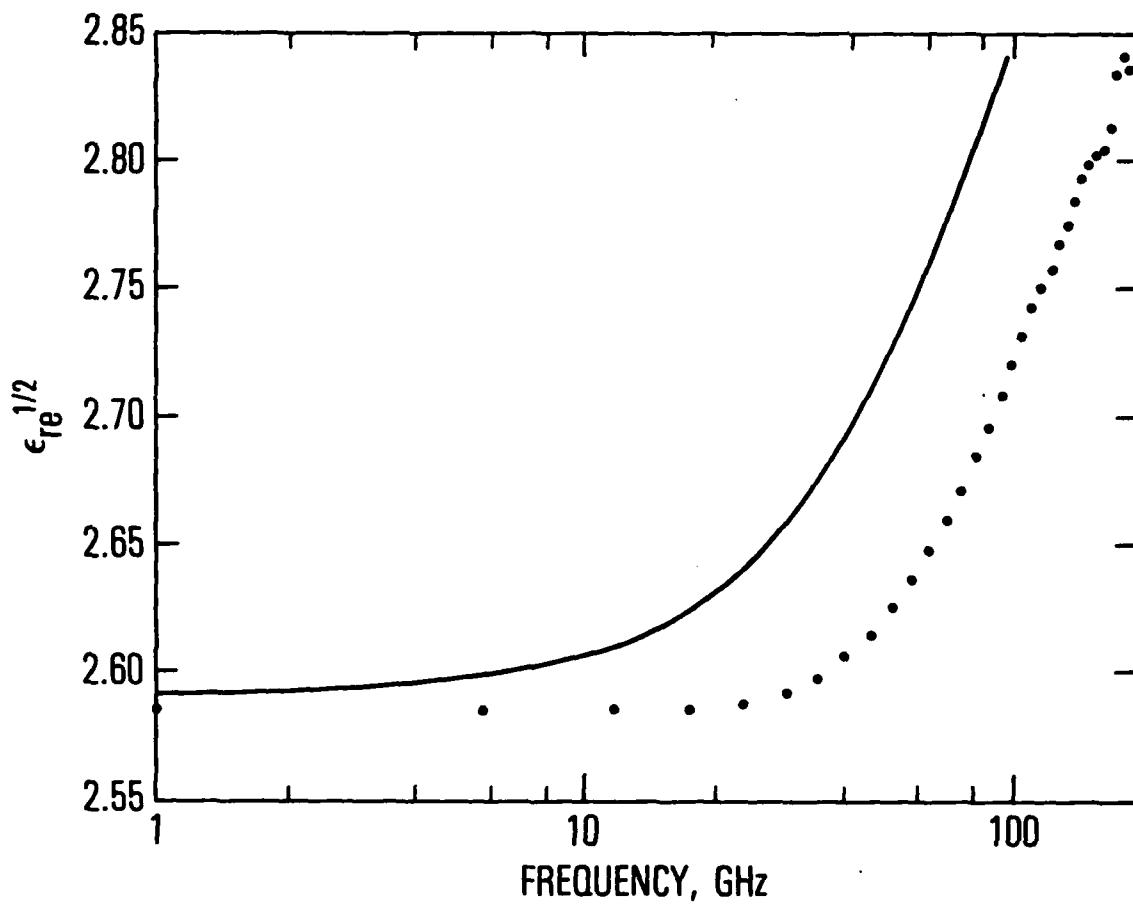


Fig. 2. Microstrip dispersion curves: solid line is calculated curve (Ref. 5); points are derived from Fourier analysis of experimental data.

## V. SUMMARY

The dispersion of short electrical pulses on microstrip lines was investigated with picosecond optoelectronic techniques, the temporal resolution of which enabled the microstrip dispersion curve to be measured with a 150-GHz bandwidth. The results indicate that the dispersion of the relatively small microstrips used in this work was significantly less than expected from previous studies.

## REFERENCES

1. P. R. Smith, D. H. Auston, and W. M. Augustyniak, Appl. Phys. Lett. **39**, 739 (1981).
2. R. P. Owens, J. E. Aitken, and T. C. Edwards, IEEE Trans. Microwave Theory Tech. **MTT-24**, 499 (1976).
3. O. P. Jain, V. Makies, and W. J. Chudobiak, Electron. Lett. **7**, 405 (1971).
4. K. K. Li, G. Arjavalingam, A. Dienes, and J. R. Whinnery, IEEE Trans. Microwave Theory Tech. **MTT-30**, 1270 (1982).
5. E. Yamashita, K. Atsuki, and T. Ueda, IEEE Trans. Microwave Theory Tech. **MTT-27**, 1036 (1979).
6. D. H. Auston, IEEE J. Quantum Electron. **QE-19**, 639 (1983).
7. K. C. Gupta, R. Garg, and I. J. Bahl, Microstrip Lines and Slotlines, Artech, Dedham, Massachusetts (1979).
8. R. Bracewell, The Fourier Transform and Its Application, McGraw-Hill, New York (1965).

## LABORATORY OPERATIONS

The Laboratory Operations of The Aerospace Corporation is conducting experimental and theoretical investigations necessary for the evaluation and application of scientific advances to new military space systems. Versatility and flexibility have been developed to a high degree by the laboratory personnel in dealing with the many problems encountered in the nation's rapidly developing space systems. Expertise in the latest scientific developments is vital to the accomplishment of tasks related to these problems. The laboratories that contribute to this research are:

Aerophysics Laboratory: Launch vehicle and reentry fluid mechanics, heat transfer and flight dynamics; chemical and electric propulsion, propellant chemistry, environmental hazards, trace detection; spacecraft structural mechanics, contamination, thermal and structural control; high temperature thermomechanics, gas kinetics and radiation; cw and pulsed laser development including chemical kinetics, spectroscopy, optical resonators, beam control, atmospheric propagation, laser effects and countermeasures.

Chemistry and Physics Laboratory: Atmospheric chemical reactions, atmospheric optics, light scattering, state-specific chemical reactions and radiation transport in rocket plumes, applied laser spectroscopy, laser chemistry, laser optoelectronics, solar cell physics, battery electrochemistry, space vacuum and radiation effects on materials, lubrication and surface phenomena, thermionic emission, photosensitive materials and detectors, atomic frequency standards, and environmental chemistry.

Computer Science Laboratory: Program verification, program translation, performance-sensitive system design, distributed architectures for spaceborne computers, fault-tolerant computer systems, artificial intelligence and microelectronics applications.

Electronics Research Laboratory: Microelectronics, GaAs low noise and power devices, semiconductor lasers, electromagnetic and optical propagation phenomena, quantum electronics, laser communications, lidar, and electro-optics; communication sciences, applied electronics, semiconductor crystal and device physics, radiometric imaging; millimeter wave, microwave technology, and RF systems research.

Materials Sciences Laboratory: Development of new materials: metal matrix composites, polymers, and new forms of carbon; nondestructive evaluation, component failure analysis and reliability; fracture mechanics and stress corrosion; analysis and evaluation of materials at cryogenic and elevated temperatures as well as in space and enemy-induced environments.

Space Sciences Laboratory: Magnetospheric, auroral and cosmic ray physics, wave-particle interactions, magnetospheric plasma waves; atmospheric and ionospheric physics, density and composition of the upper atmosphere, remote sensing using atmospheric radiation; solar physics, infrared astronomy, infrared signature analysis; effects of solar activity, magnetic storms and nuclear explosions on the earth's atmosphere, ionosphere and magnetosphere; effects of electromagnetic and particulate radiations on space systems; space instrumentation.

**END**

**FILMED**

**1-86**

**DTIC**